Numerical analysis of concrete filled steel tube columns with plain and steel fiber reinforced concrete infill

Authors: Kingsley Ukanwa, G. Charles Clifton, James B.P. Lim, Stephen J. Hicks, Umesh K. Sharma

Abstract

In recent years, concrete filled steel tubes have become popular among structural engineers as columns in multi-storey buildings, due to their many advantages which include; high seismic resistance, high load bearing capacity, and high fire resistance without external protection. However, questions remain on aspects of their performance in ambient temperature and in severe fires. The answers to these questions lie in a mix of experimental testing and advanced numerical analysis. Any numerical model must be validated against experimental testing. In the research reported in this paper, a three dimensional nonlinear finite element model is presented and validated by a series of column tests available in the literature in order to study the structural behaviour of axially loaded concrete filled tubular (CFT) using plain concrete and steel fiber reinforced concrete as infill. The main variables for the columns were its cross-section, slenderness, concrete compressive strength and the load eccentricity. Experimental tests have shown that at ambient temperatures, the use of steel fiber reinforced concrete as infill increases the ductility of columns and controls the crack opening width and propagation. Therefore, in this study, a sensitivity analysis has been performed to study the parameters that are influential to the ultimate bearing capacity of a concrete filled steel tube column when subjected to axial loads. Results showed that the addition of steel fibers to the concrete had little effect on the ultimate strength of the column, but increased the ductility of all the columns. The concrete compressive strength is significant to the ultimate strength of the column when the steel contribution ratio is less than 0.6 and the slenderness of the column is less than 0.62, but less influential when these 0.6 and 0.62 are exceeded respectively. The parameters that are most influential to the ultimate strength and deflection of the column are its cross sectional area and the load eccentric distance.

1.0 INTRODUCTION

Concrete filled steel tube (CFST) columns have become popular amongst engineers and designers in recent years due to their advantage of having a high compression capacity, good ductility for high seismic resistance, reduction in size of the column, ease of construction and considered high fire resistance (Zhao, Han, & Lu, 2010). CFST are used in many structural applications including columns supporting platforms of offshore structures, roofs of storage tanks, bridge piers, piles, and columns in seismic zones. However, due in part to the 1995 Kobe earthquake in Japan, the emphasis on concrete filled steel tube composite column construction was no longer on its structural strength, but rather on its ductility, energy absorption and performance for use in seismic zones (Kitada, 1998). Steel tube local buckling is the most critical issue to consider when designing a steel tube column. Therefore, researchers have indicated that addition of concrete infill to the steel tube will reduce the effects of local buckling (Brauns, 1998; Ellobody, Young, & Lam, 2006). Among the various materials used, steel fiber reinforced concrete is becoming popular as the use for infill due to its high tensile strength, low shrinkage, high flexural strength, high ductility and energy absorption as indicated by Ehab and Zhao et.al (Ehab, 2013; Zhao, Lok, Li, & Lim, 2001) without the physical constraints of having to put longitudinal and transverse reinforcement into the concrete core. Comprehensive experimental and numerical experiments conducted by Zeghiche & Chaoui (Zeghiche & Chaoui, 2005) and Johansson & Gylltoft (Johansson & Gylltoft, 2001) respectively, showed that it is possible to achieve ductility in the column by also using high strength concrete. However, it will be more useful to use a thicker steel tube when using a high strength concrete as opposed to normal strength concrete when the ductility of a column is the main concern. Ehab (Ehab, 2013), concluded that the addition of fiber to plain concrete increases its flexural and tensile strength which results in superior post-elastic material properties. There are various parameters that affect the behaviour of steel fiber reinforced concretes which includes its matrix strength, fiber type, fiber Young's modulus, fiber volume and fiber strength.

---

[1]PhD Candidate, Dept. of Civil Engineering, University of Auckland, Auckland, New Zealand. ukanwakingsley@gmail.com
[2]Associate Professor, Dept. of Civil Engineering, University of Auckland, Auckland, New Zealand
[3]Senior Lecturer, Dept. of Civil Engineering, University of Auckland, Auckland, New Zealand
[4]General Manager, Heavy Engineering Research Association, Auckland, New Zealand
[5]Associate Professor, Dept. of Civil Engineering, Indian Institute of Technology Roorkee, Uttarakhand, India

Figs. 1a and b shows a comparison between the stress, strain curve of plain and steel fiber reinforced concrete. The influence of steel fiber l/d ratio is also important to determine the stress - strain values.

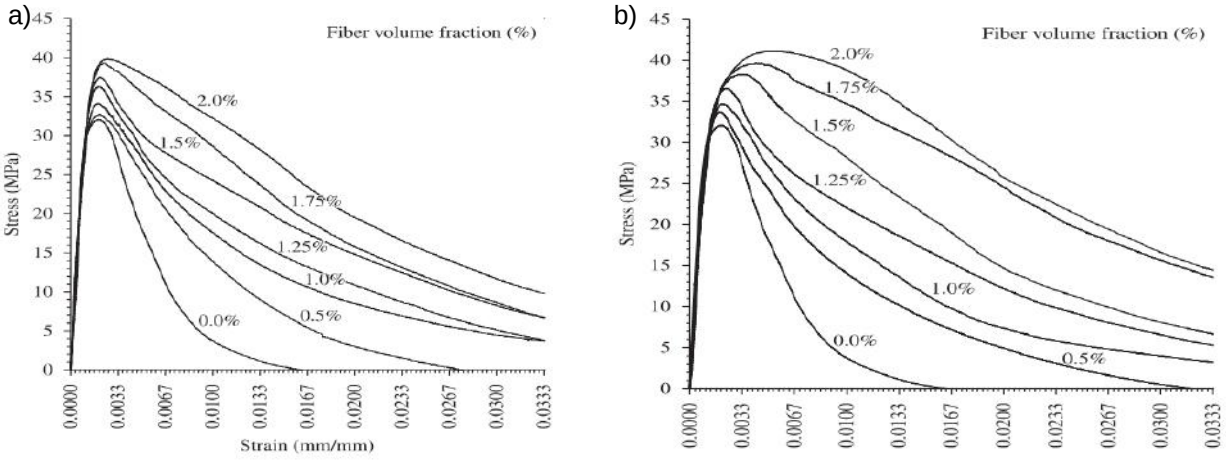

Fig.1: a) l/d ratio of 60, fiber fraction. b) l/d ratio of 75, fiber fraction (Marara, Eren, & Yitmena, 2011)

Tokgoz & Dundar (Tokgoz & Dundar, 2010) conducted experimental tests on 16 concrete filled steel tubular columns with plain and steel fiber reinforced concrete infill. The columns were loaded axially with different levels of eccentricity having e/D ratio given in Table 2 where e is the eccentricity and D is the depth of the column. It was reported that the inclusion of steel fibers to the concrete improved the ductility and deformation of the column; however, it had little effect on the ultimate strength capacity of the column. Gopal & Manoharan (Gopal & Manoharan, 2006), carried out tests on 12 slender circular steel tubular columns filled with both plain and steel fiber reinforce concrete, the specimens were tested under eccentric axial loading to investigate the effects of fiber reinforced concrete on the ultimate strength and behaviour of the composite columns. It was reported that the use of fiber reinforced concrete as infill for tubular steel gives the column additional strength and ductility.

The main objective of the study reported herein has been to investigate numerically the behaviour of axially loaded steel fiber reinforced CFST and validate the model by comparison with experimental data available in the literature. Sixteen (16) composite columns were simulated from the literature and the main variables for the columns were its cross-section, slenderness, concrete compressive strength and the load eccentricity. The ultimate strength and load-deflection profile of the column were analysed and compared to the experimental results.

2.0 Finite Element Modelling

2.1 General

In this study, a three dimensional non-linear finite element analysis was employed using ABAQUS SIMULIA (ABAQUS, 2009) to analyse the behaviour of plain and steel fiber reinforced CFST column. The experimental tests were carried out by Tokgoz & Dundar (Tokgoz & Dundar, 2010). The model was developed in three parts, as shown in Fig. 2. The first part to be modelled was the steel tube followed by the concrete infill and thirdly the end-plates where the axial load of the column was applied in an eccentric distance. A total of 16 CFST columns were modelled, the material properties and geometry of the columns were obtained from experimental tests carried out in the literature which are summarized in Tables 1 and 2 where the slenderness (λ) and steel ratio (δ) were also recorded. The CFST models were classified into 4 sets, CFSTC-I and CFSTC-II were modelled using different concrete mix proportion, while a 0.75% volume of steel fiber was added to model CFSTC-I-SF and CFSTC-II-SF. All sets of concrete classification had 60 x 60 x 5 mm^3, 70 x 70 x 5 mm^3, 80 x 80 x 4 mm^3 and 100 x 100 x 4 mm^3 cross sectional area. The total lengths of all columns were 1250 mm.

2.2 Finite element mesh and geometry

The main parameters of the model are the column breadth (B), the depth (D), the steel tube thickness (t) and the loading eccentricity (e). The Steel fiber and plain CFST columns were modelled using shell and solid elements available in the ABAQUS SIMULIA material definition library (ABAQUS, 2009).

The steel tube consisted of four-nodded quadrilateral shell element (S4R) mesh while eight-nodded solid elements (C3D8R) with reduced integration were used in modelling the concrete core. The loading end plate was modelled as discrete rigid (R3D4) which will enable evenly stress distribution of the eccentric axial load to the column.

2.3. Boundary Condition and Column Loading

The testing procedure conducted by Tokgoz & Dundar (Tokgoz & Dundar, 2010) was used to model the boundary condition and load application of the CFST column. The column was modelled with a pin-pin end condition. A reference point was created on the loading plate to indicate the position of the e_x and e_y eccentric distance of the applied load. Figs 3 and 4 show the experimental setup and numerical assembly of the CFST columns respectively.

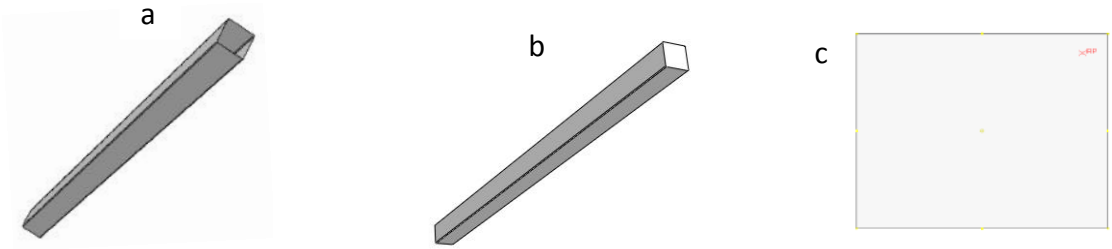

Figures 2: a). Steel tube. b). Concrete core. c). End plate

Table 1: Concrete Densities for CFST column

Specimen	Gravel (Kg/m^3)	Sand (Kg/m^3)	Cement (Kg/m^3)	Water (Kg/m^3)	Plasticizer (Kg/m^3)	Steel Fiber (Kg/m^3)	Density (Kg/m^3)
CFSTC-I	1140	750	400	140	4	-	2343
CFSTC-II	1130	740	400	130	8	-	2408
CFSTC-I-SF	1130	740	400	140	4	58.88	2473
CFSTC-II-SF	1120	730	400	130	8	58.88	2447

Table 2: CFST column specimen parameters

Specimen	B x D x t (mm)	B/t	e/D	L/D	λ	δ	fc (MPa)	E_{cm} (GPa)	e_x (mm)	e_y (mm)
CFSTC-I	60 x 60 x 5	12	0.5	20.8	0.76	0.71	51.48	41.24	30	30
	70 x 70 x 5	14	0.5	17.86	0.66	0.67	51.48	41.24	35	35
	80 x 80 x 4	20	0.5	15.63	0.59	0.57	51.48	41.24	40	40
	100 x 100 x 4	25	0.5	12.5	0.48	0.51	51.48	41.24	50	50
CFSTC-I-SF	60 x 60 x 5	12	0.5	20.8	0.77	0.70	54.13	41.77	30	30
	70 x 70 x 5	14	0.5	17.86	0.66	0.66	54.13	41.77	35	35
	80 x 80 x 4	20	0.5	15.63	0.60	0.56	54.13	41.77	40	40
	100 x 100 x 4	25	0.5	12.5	0.49	0.49	54.13	41.77	50	50
CFSTC-II	60 x 60 x 5	12	0.67	20.8	0.77	0.69	56.24	42.17	40	40
	70 x 70 x 5	14	0.64	17.86	0.67	0.65	56.24	42.17	45	45
	80 x 80 x 4	20	0.63	15.63	0.60	0.55	56.24	42.17	50	50
	100 x 100 x 4	25	0.6	12.5	0.49	0.48	56.24	42.17	60	60
CFSTC-II-SF	60 x 60 x 5	12	0.67	20.8	0.77	0.69	58.67	42.67	40	40
	70 x 70 x 5	14	0.64	17.86	0.67	0.64	58.67	42.67	45	45
	80 x 80 x 4	20	0.63	15.63	0.61	0.54	58.67	42.67	50	50
	100 x 100 x 4	25	0.6	12.5	0.50	0.47	58.67	42.67	60	60

2.4. Material modelling of steel tube

The stress-strain relations for steel tubes are taken from values used in the experimental tests conducted by Tokgoz & Dundar (Tokgoz & Dundar, 2010). The material properties of the steel tubes were modelled in ABAQUS (ABAQUS, 2009) as having a modulus of elasticity of 200GPa and Poissons ratio of 0.3. The steel tube was modelled using (*PLASTIC option) the recorded yield stress given as 290MPa. Properties of the steel in the post-yielding range were 430MPa.

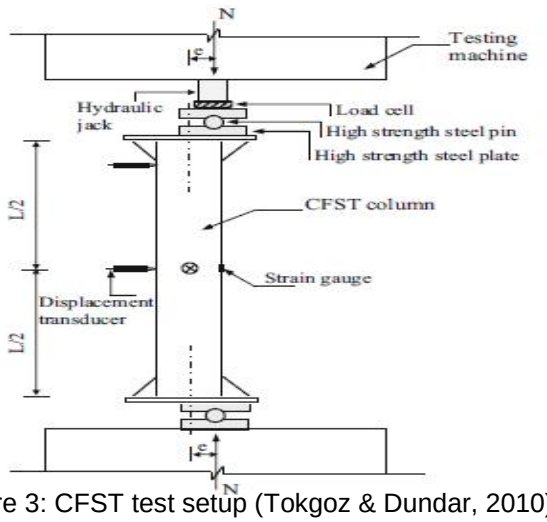

Figure 3: CFST test setup (Tokgoz & Dundar, 2010)

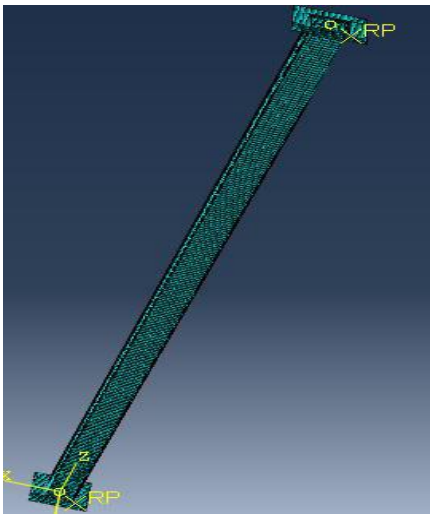

Figure 4: CFST Numerical Setup

2.5 *Material modelling of steel fiber*

The steel fiber dosage used in the model was 0.75% volume as specified in the experimental tests. The material geometry of the steel fiber is given in table 3. There are various approaches to modelling steel fiber into the concrete as described in the literature. Experimental research carried out by Musmar (Musmar, 2013) indicates that addition of steel fiber to the concrete will have an effect on the tensile strength and ductility of the concrete. Musmar proposed Eq. 1 to determine the value of the tensile strength of the concrete. This was used in this study to model the fiber reinforced concrete.

Table 3: Steel Fiber Geometry

S.F Type	Density (kg/m^3)	%volume	Length (mm)	Diameter (mm)
RC 65/35 BN	7850	0.75%	35	0.55

$$f_{sp} = (0.6 + 0.4\left(v_f \times \frac{L}{d}\right)) \times \sqrt{f_c'} \quad (1)$$

Where v_f is the fiber volume, L = length of fiber, d = diameter of fiber and f_c' is the compressive strength of concrete.

2.6 Modelling of confined concrete

The approach used in modelling the effects of confinement of the plain and steel fiber reinforced concrete was similar to the approach used by Dai & Lam (Dai & Lam, 2010). Fig. 5 shows the equivalent uniaxial presentation for the stress-strain curve of confined and unconfined concrete. In this figure f_c is the unconfined concrete cylindrical compressive strength which is equal to 0.8fcu; where f_{cu} is the cube compressive strength of the unconfined concrete. The unconfined strain ($\underline{\varepsilon}_c$) value is taken as 0.003 for plain concrete as recommended by the ACI Specification (ACI, 2008). f_{cc} and $\underline{\varepsilon}_{cc}$ are the confined concrete compressive strength and confined stain respectively, which can be derived from Eqs. 2 and 3, respectively, proposed by Mander et.al (Mander, Priestley, & Park, 1988).

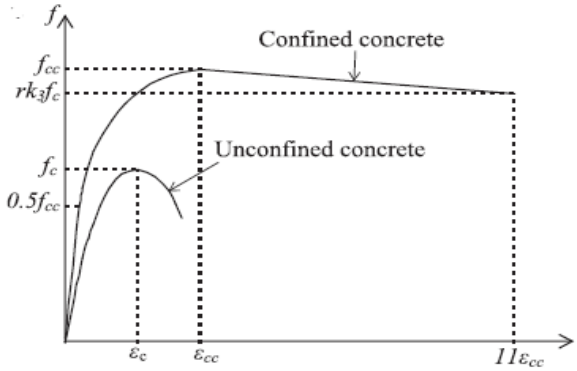

Figure 5: Confined concrete stress strain curve (Ellobody & Young, 2006)

$$f_{cc} = f_c + k_1 f_l \quad (2)$$

$$\varepsilon_{cc} = \varepsilon_c \left(1 + k_2 \frac{f_l}{f_c}\right) \quad (3)$$

Where f_l = lateral confining pressure from the steel tube section.

$$f_l = \frac{2\sigma_\theta t}{D} \quad (4)$$

Where $\sigma_\theta = 0.1 f_y$ proposed by Mander et.al (Mander, Priestley, & Park, 1988). The factors k_1 and k_2 in Eqs. 2 and 3 are taken as 4.1 and 20.5 respectively, as given by Richart et al. (Richart, Brandzaeg, & Brown, 1928). The Equivalent stress–strain curves of unconfined and confined concrete are expressed in three parts. The first part defines the initial limit stress, which is taken as $0.5 f_{cc}$ as given by Hu et al. (Hu, Huang, Wu, & Wu, 2003). The young's modulus of confined concrete is calculated using the empirical formula provided in the ACI code (ACI, 2008), given in Eq. 5.

$$E_{cc} = 4700 \sqrt{f_{cc}} \ \ Mpa \quad (5)$$

Where f_{cc} is the strength of confined concrete. The Poisson's ratio of confined concrete is taken as 0.2 as given in Eurocode 2 (Eurocode 2, 2004). The second part defines the nonlinear portion of the stress-strain curve starting from the proportional limit stress $0.5 f_{cc}$ to the confined strength of the concrete f_{cc}. This part of the curve was proposed by Saenz (Saenz, 1964) and can be determined from Eq. 6.

$$f = \frac{E_{cc}\varepsilon}{1+(R+R_E-2)\left(\frac{\varepsilon}{\varepsilon_{cc}}\right)-(2R-1)\left(\frac{\varepsilon}{\varepsilon_{cc}}\right)^2+R\left(\frac{\varepsilon}{\varepsilon_{cc}}\right)^3} \quad (6)$$

$$R_E = \frac{E_{cc}\,\varepsilon_{cc}}{f_{cc}} \quad (7)$$

$$R = \frac{R_E(R_\sigma-1)}{(R_\sigma-1)^2} - \frac{1}{R_\varepsilon} \quad (8)$$

Where the constants Rσ and Rε are equal to 4 as recommended by Hu & Schnobrich (Hu & Schnobrich, 1989).
The third part defines the descending value of the confined concrete stress–strain curve; this part starts from the maximum confined concrete strength f_{cc} to a lower value $rk_3 f_{cc}$ with a corresponding strain value of $11\varepsilon_{cc}$ as proposed by Hu et al. (Hu, Huang, Wu, & Wu, 2003).
The Concrete was modelled using the concrete damaged plasticity (CDP) model implemented in ABAQUS SIMULIA (ABAQUS, 2009) standard and explicit material library. The model provides a general analysis of concrete and other quasi-brittle material. The concrete damaged plasticity model uses stress-strain relationships to correlate parameters for relative concrete damage for both tension and compression under uni-axial loading as shown in Figs. 6a and 6b.

$$D = 1 - \left(\frac{E}{E_o}\right) \quad (8)$$

Where, D is the damage parameter of concrete in compression and tension, E_0 is the initial (undamaged) elastic stiffness of the material, E is the damaged elastic stiffness of the confined concrete and d_t and d_c are the damage indices of concrete in tension and compression. The assumptions are made that the concrete will take a compression load even after tension cracking, but will not take tension load after compression crushing. Eq. 8 was used in calculating the damage parameters under uni-axial tension and compression.

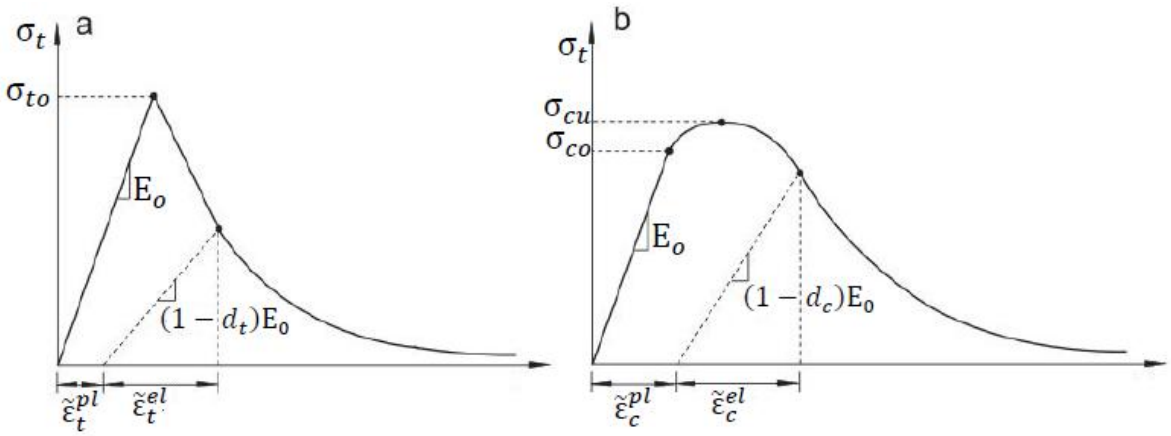

Figures 6: a) Damage plasticity tension b).Damage plasticity compression (ABAQUS, 2009)

2.7 Concrete – Steel tube interface

The end-plates were included in the model to achieve equal shortening of the entire column column and to model the experiemental test setup used to put load into the columns at each end.. The interactions between the steel and concrete were modelled as a general contact, where the steel tube acted as the master surface and the concrete the slave surface. A master surface can penetrate the slave surface, but the slave surface cannot penetrate the master surface. The surface interactions were modelled in such a way that the friction between the two faces is maintained throughout when in contact. The coefficient of friction between the steel tube and concrete surfaces was taken as 0.2 from parametric studies carried out.

3.0 Results and Discussion

Concrete filled steel tube column ultimate axial load is calculated by adding the ultimate strengths of its individual members. When the load is applied at an eccentric distance, it is very important to take into account the distance of eccentricity when calculating the ultimate strength of the column. The ultimate loads obtained from the finite element (P_{FEA}) analysis, laboratory experiments (P_{EXP}) and Theoretical (P_{THY}) analysis are reported in Table 4. The finite element analysis result of the ultimate strength of the column is compared to the experimental and theoretical results. The comparison indicated a good correlation between the experimental results and the numerical analysis results while the theoretical result was more conservative. The various parameters that contributed to the ultimate load of the column are the thickness, cross section of the column, concrete compressive strength, load eccentricity and the tensile strength of the concrete. The moment (M) of the column at mid height was calculated using the equation $M = P \times (e + d)$ where P is the ultimate load, e is the eccentric distance and d is the deflection at mid height.

Table 4: Finite element analysis, experimental and theoretical comparison of CFST column

Model No.	P_{FEA} (KN)	P_{EXP} (KN)	P_{THY} (KN)	M_{FEA} (kN.m)	M_{EXP} (kN.m)	$\frac{P_{EXP}}{P_{FEA}}$	$\frac{P_{THY}}{P_{FEA}}$	$\frac{M_{EXP}}{M_{FEA}}$
CFSTC-I-60	140.66	128	115.77	4.50	4.48	0.910	0.823	0.996
CFSTC-I-SF-60	142.90	124	115.35	4.59	4.50	0.868	0.807	0.980
CFSTC-II-60	105.39	97	93.21	4.46	4.60	0.920	0.884	1.031
CFSTC-II-SF-60	107.44	104	93.73	4.54	4.63	0.968	0.872	1.020
CFSTC-I-70	161.62	168	150.28	6.08	6.41	1.039	0.930	1.054
CFSTC-I-SF-70	167.19	174	151.24	6.34	6.46	1.041	0.905	1.019
CFSTC-II-70	133.15	142	124.61	6.53	6.61	1.066	0.936	1.012
CFSTC-II-SF-70	136.55	148	125.35	6.74	6.65	1.084	0.918	0.987
CFSTC-I-80	159.50	173	163.22	6.83	7.65	1.085	1.023	1.120
CFSTC-I-SF-80	187.75	175	165.07	8.30	7.90	0.932	0.879	0.952
CFSTC-II-80	144.16	147	137.52	8.08	7.87	1.020	0.954	0.974
CFSTC-II-SF-80	152.72	156	138.42	8.26	7.92	1.021	0.906	0.959
CFSTC-I-100	231.32	245	233.78	12.32	12.99	1.059	1.011	1.054
CFSTC-I-SF-100	246.51	248	236.22	13.95	13.13	1.006	0.958	0.941
CFSTC-II-100	207.05	218	202.52	13.42	13.33	1.053	0.978	0.993
CFSTC-II-SF-100	214.84	222	204.14	13.90	13.44	1.033	0.950	0.967
Mean						**1.007**	**0.921**	**1.004**
Standard Deviation						**0.067**	**0.060**	**0.046**

The rest of this section discusses the importance of the various parameters studied.

Steel tube thickness

The steel tube thickness is an important parameter that determines the behaviour and buckling mode of the CFST column. All 16 columns failed due to the local buckling of the steel tube. For columns having a thickness of 4mm, there was an uneven distribution of stress during the early stages of load application which resulted in a premature plastic deformation at the top perpendicular to the eccentric loading direction of the steel tube. There was a drop in the column strength of the CFST-II-80 column at a deflection of 2.02 mm before it reached its ultimate strength value and this was due to the premature plastic deformation of the steel tube. Fig 7 shows the load deflection curve of CFST-II-70 and CFSTC-II-80 while Fig 8 shows the premature brittle fracture of CFSTC-II-80.

Cross Section of the column

The column's cross sectional area was the most important factor that governed the axial strength of the column. As shown in Table 4, an increase in the columns cross section area resulted in an increase in its ultimate strength. The maximum moment values of columns with larger cross sectional area were more than columns having a smaller cross sectional area and this was mainly due to the length to depth ratio of the columns and eccentric distance.

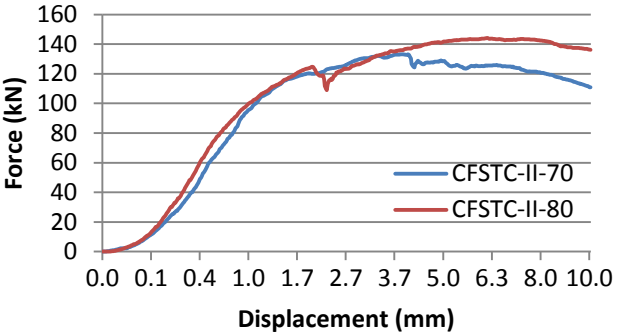

Figure 7: Effectiveness of steel tube thickness

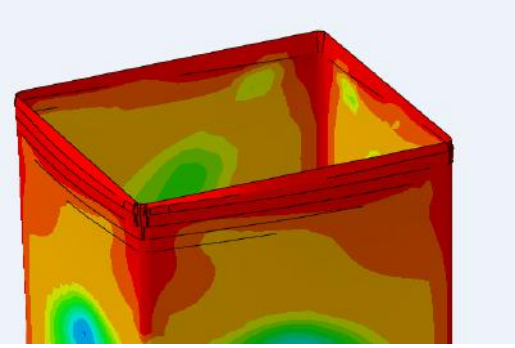

Figure 8: Steel tube ductile fracture

Concretes compressive strength and steel contribution ratio

The compressive strength of the concrete on a column with a larger steel contribution ratio had little effect on the ultimate strength of the column. There was only 2% increase in ultimate strength for similar columns with varying concrete compressive strength. However, the columns with less steel contribution ratio had a larger difference in the ultimate strength recorded. This indicates that the compressive strength of concrete is significant for columns having a smaller steel contribution ratio. Figs 9 a & b shows the comparison of columns with high steel contribution ratio, while Figs 9 c & d shows a comparison of columns with lower steel contribution ratio.

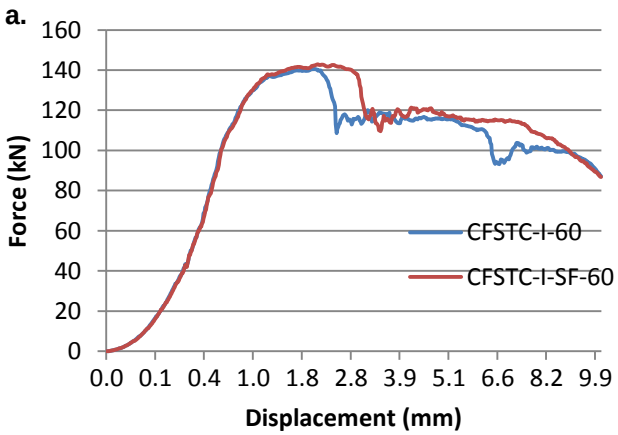

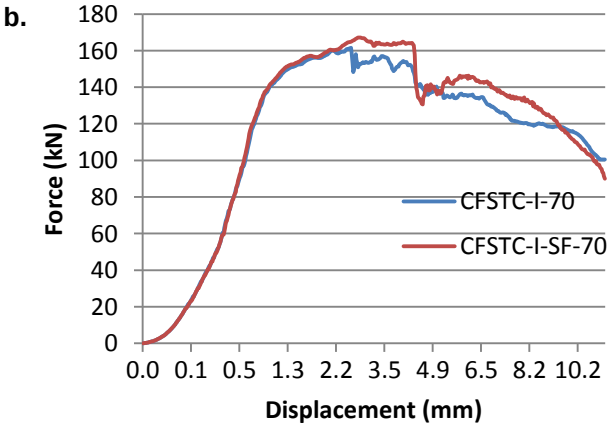

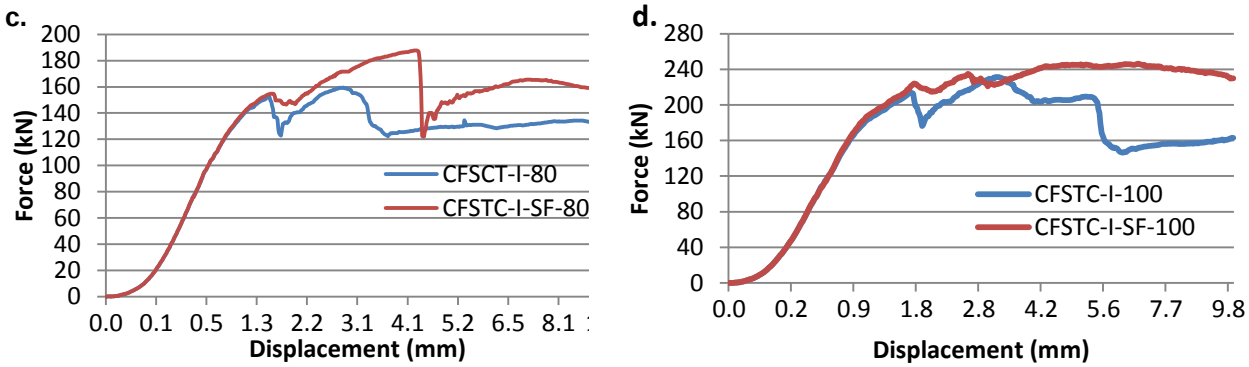

Figure 9 (a-d): Effectiveness of compressive strength and steel contribution ratio.

Load Eccentricity

The e/D ratio of the column was a contributing factor to the ultimate strength and moment of the column. For columns having a 30% increase in e/D ratio, there is a corresponding 33% reduction in the ultimate axial strength of the column. The moment values were significantly increased by columns having a lower steel contribution ratio. Figs 10a & b gives a graphical illustration of the significance of e/D ratio.

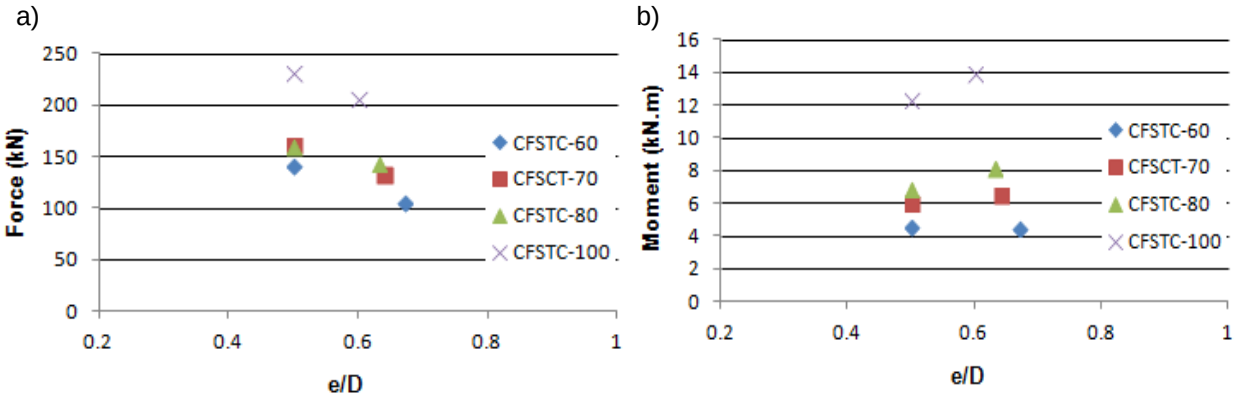

Figure 10: a) effect of e/D to ultimate axial strength b) effect of e/D to moment value

4. Conclusion

The computational finite element modelling of concrete filled steel tubes with plain and steel fiber reinforced concrete infill is presented in this study. There was a good agreement between the FEA results and experimental results presented in Table 4 and shown graphically in Fig 11.

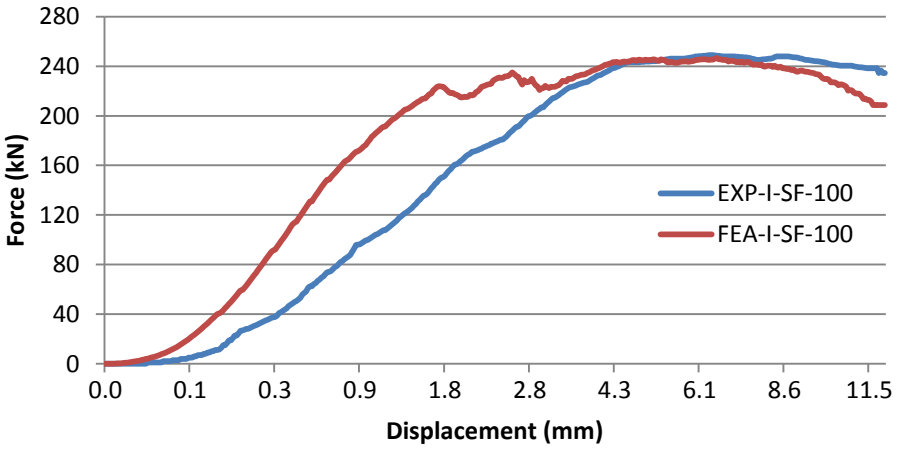

Figure 11: Comparison of FEA and experimental result

The concrete compressive strength is not very significant for columns having a higher steel contribution ratio. The addition of steel fiber to the concrete had little effect on the ultimate strength of the column. However the crack propagation of the concrete core affected the ductility of the column. Figs 12 a & b shows the concrete tensile damage of CFSTC-I-60 and CFSTC-I-SF-60 at an axial load of 100kN. This indicates that for concrete with steel fiber reinforcement, the concrete core will be able to delay the local buckling of the column for a longer period and this gives the columns a better ductility than when plain concrete are used as infill. This is important when the columns are designed to have a better ductility in seismic zones.

a. b.

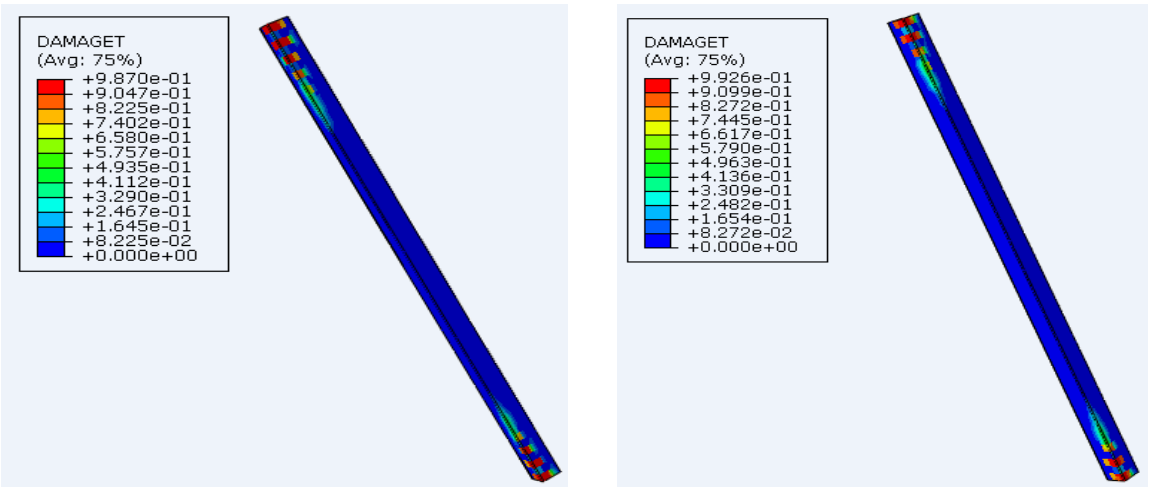

Figure 12: a) Tensile Damage of CFSTC-I-60 b) Tensile damage of CFSTC-I-SF-60

Acknowledgements

The authors wish to express gratitude to the Heavy Engineering Educational & Research Foundation (HEERF) for their doctoral scholarship support. The authors also acknowledge the contribution of NeSI high-performance computing facilities to the results of this research. NZ's national facilities are provided by the NZ eScience Infrastructure and funded jointly by NeSI's collaborator institutions and through the Ministry of Business, Innovation & Employment's Research Infrastructure programme.

References

ABAQUS. (2009). Analysis user's manuals and example problems manuals. *version 6.9*. Rhode Island, Providence: Abaqus Inc.

ACI. (2008). *Building code requirements for structural concrete and Commentary.* Detroit: American Concrete Institute.

Brauns, J. (1998). Analysis of stress state in concrete-filled steel column. *Journal of Construct Steel Research, 49*(2), 189-196.

Dai, X., & Lam, D. (2010, March). Numerical modelling of the axial compressive behaviour of short concrete-filled elliptical steel . *Journal of Constructional Steel Research, 66*(7), 931–942. doi:10.1016/j.jcsr.2010.02.003

Ehab, E. (2013). Numerical modelling of fiber reinforced concrete-filled stainless steel tubular columns. *Thin-Walled Structures, 63*, 1-12.

Ellobody, E., & Young, B. (2006). Design and behaviour of concrete-filled cold-formed stainless steel tube columns. *Engineering Structures, 28*, 716–728. doi:10.1016/j.engstruct.2005.09.023

Ellobody, E., Young, B., & Lam, D. (2006). Behavior of Normal and High Strength Concrete-Filled Compact Steel Tube Circular Stub Columns. *Journal of Constructional Steel Research, 62*, 706–715.

Eurocode 2. (2004). Design of Concrete Structures. *BS EN 1992-1-1:2004*.

Gopal, S. R., & Manoharan, p. D. (2006). Experimental behaviour of eccentrically loaded slender circular hollow steel columns in-filled with fiber reinforced concrete. *Journal of Constructional Steel Research, 62*, 513–520.

Hu, H. T., & Schnobrich, W. C. (1989). Constitutive modeling of concrete by using nonassociated plasticity. *Journal of Materials in Civil Engineering, 1*(4), 199–216.

Hu, H.-T., Huang, C.-S., Wu, M.-H., & Wu, Y.-M. (2003). Nonlinear Analysis of Axially Loaded Concrete-Filled Tube Columns with Confinement Effect. *JOURNAL OF STRUCTURAL ENGINEERING, 129*(10), 1322-1329.

Johansson, M., & Gylltoft, K. (2001). Structural behaviour of slender circular steel concrete composite columns under various means of load application. *Steel and Composite Structures, 1*(4), 393-410.

KKitada, T. (1998, June 18). Ultimate strength and ductility of state-of-the-art concrete-filled steel bridge piers in Japan. *Engineering Structures, 20*(4-6), 347-354. doi:10.1016/S0141-0296(97)00026-6

Mander, J. B., Priestley, M. J., & Park, R. (1988). Theoretical stress–strain model for confined concrete. *Journal of Structural Engineering, 114*(8), 1804–1826.

Marara, K., Eren, Ö., & Yitmena, İ. (2011, May). Compression Specific Toughness of Normal Strength Steel Fiber Reinforced Concrete (NSSFRC) and High Strength Steel Fiber Reinforced Concrete (HSSFRC). *Materials Research, 14*(2), 239-247. doi:10.1590/S1516-14392011005000042

Musmar, M. (2013). Tensile Strength of Steel Fiber Reinforced Concrete. *Contemporary Engineering Sciences, 6*(5), 225 - 237. doi:http://dx.doi.org/10.12988/ces.2013.3531

Richart, F. E., Brandzaeg, A., & Brown, R. L. (1928). *A study of the failure of concrete under combined compressive stresses.* University of Illinois Engineering Experimental Station. Champaign (IL, USA): Bull 185.

Saenz, L. P. (1964). Discussion of “Equation for the stress–strain curve of concrete” by P. Desayi, and S. Krishnan. *Journal of the American Concrete Institute , 61*, 1229–1235.

Tokgoz, S., & Dundar, C. (2010). Experimental study on steel tubular columns in-filled with plain and steel fiber reinforced concrete. *Thin-Walled Structures, 48*, 414-422. doi:10.1016/j.tws.2010.01.009

Zeghiche, J., & Chaoui, K. (2005). An experimental behaviour of concrete-filled steel tubular columns. *Journal of Constructional Steel Research, 60*(1), 53-66.

Zhao, P. J., Lok, T. S., Li, X. B., & Lim, C. H. (2001). Behavior of steel fiber reinforced concrete under dynamic load. *Proceedings of 4th Asia-Pacific conference on shock and impact loads on structures*, (pp. 573–80). Singapore.

Zhao, X. L., Han, L. H., & Lu, H. (2010). *Concrete-Filled Tubular Members and Connections.* London: Spoon Press.